JOURNAL OF MATERIALS SCIENCE **40** (2005) 4299–4306

Carbothermic reduction of zinc sulfide in the presence of calcium oxide

C. H. HUANG, C. I. LIN
Department of Chemical Engineering, National Taiwan University of Science and Technology, Taipei, Taiwan 106

H. K. CHEN
Department of Chemical Engineering, Hwa-Hsia College of Technology and Commerce, Taipei, Taiwan 235

The carbothermic reduction of zinc sulfide in the presence of calcium oxide has been studied using X-ray diffractometry (XRD), scanning electron microscopy (SEM) and surface area measurements. The results of XRD indicated that zinc sulfide was first transformed from β type to α type, then reacted to give an intermediate product of zinc oxide before being reduced finally to zinc vapor. The sulfur of zinc sulfide was scavenged as calcium sulfide which remained in the solid, and carbon black formed carbon monoxide. SEM showed that the zinc containing particles and carbon grains shrank gradually; the calcium containing grains swelled and sintered during the reaction. The surface area of the solid sample decreased drastically in the initial stage and then increased with reaction time; the pore volume of the solid sample was also reduced much faster initially and then increased slowly. The average pore diameter, however, increased remarkably in the initial stage, decreased and then leveled off. These results were explained by considering the phase transformation of zinc sulfide, escape of zinc vapor, gasification of carbon and expansion and sintering of calcium sulfide. A reaction mechanism and model are proposed to explain the variations in chemical composition and physical properties of the solid sample during the reaction.

1. Introduction

Carbon and lime (or limestone) are normally added in the process of recovering zinc from zinc sulfide ore at elevated temperatures. Carbon acts as a reducing agent and lime (or limestone), a scavenging agent to fix the sulfur in the ore to prevent the emission of sulfur dioxide due to the oxidation of the ore. The main reaction involved in this process is [1]

$$\mathrm{ZnS(s) + CaO(s) + C(s) = Zn(g) + CaS(s) + CO(g)} \quad (1)$$

A zinc oxide pellet is commonly employed in the steam reforming process to absorb hydrogen sulfide. After a certain period, part of zinc oxide is transformed to zinc sulfide and can absorbs no more hydrogen sulfide. The pellet thus produced is called spent zinc oxide catalyst or spent catalyst. It should not be discarded in landfills because it may pollute the environment. Zinc in the spent catalyst can be recovered through the carbothermic reduction process with lime (or limestone). Reaction 1 is one of the important reactions in this zinc recovery process [2].

In spite of the importance of the two processes mentioned above, not many investigations have been carried out [1, 3–6]. Out of five publications identified that referred to this reaction, the following topics have been investigated: strength of briquette for reduction [5, 6], conversion of zinc sulfide [5, 6], reaction mechanism [1, 3, 4], activation energy [1, 3] and reaction rate [1, 3, 4, 6].

Thermal gravimetric analysis (TGA) [1, 3, 4] and X-ray diffractometry (XRD) [4–6] are the most popular techniques to investigate this reaction system. Scanning electron microscopy (SEM) and surface area measurement, however, have not been found to be employed.

To understand Reaction 1 more thoroughly, the carbothermic reduction of zinc sulfide in the presence of calcium oxide under argon stream over the temperature range 1,180–1,353 K is studied. XRD is used to monitor the variation in the composition of the solid sample during reaction. An SEM and a surface area analyzer are employed to detect the structural changes of the sample. A reaction mechanism and model are developed to interpret the overall reaction based on the above experimental results.

2. Experimental procedure

2.1. Materials

Argon (Yuang-Ron Gas Co., Taipei, Taiwan) with a minimum purity of 99.99% was employed. Zinc sulfide (reagent grade, minimum purity of 99.99%)

and calcium oxide (reagent grade, minimum purity of 99.99%) were supplied by Cerac Chem. Co. (Milwaukee, WI) while carbon black (reagent grade, minimum purity of 99.99%) was obtained from Strem Chem. Co. (Newburyport, MA).

2.2. Sample preparation

Zinc sulfide and carbon black were dried separately at 378K for 43,200 s (12 h). Zinc sulfide and calcium oxide were employed with their original particle sizes while carbon black was screened to obtain the size of 67.7×10^{-6}m (size range: $61 \times 10^{-6} - 74 \times 10^{-6}$ m). Carbon black was then dried at 378 K for 43,200 s (12 h) again. These solid reactants at predetermined ratios were mixed in a V-type blender (S-2, Tsutsui Scientific Instruments, Tokyo , Japan) for 21,600 s (6 h) thereafter. The powder mixture thus produced was then transferred into a bottle stored in a vacuum drier.

2.3. Carbothermic reduction

Carbothermic reduction was carried out in a TGA. The system was heated from room temperature with a steady flow of argon. As the temperature reached the predetermined value and maintained stable for 1,800 s (0.5 h), the system was opened for positioning the crucible (0.02 m diameter and 0.03 m height) loaded with sample (0.4756×10^{-3} kg) and then closed. The reaction then started isothermally. The pressure in the system was maintained at 19.6 to 39.2 Pa above atmospheric during the reaction. The solid sample was removed and quenched in an argon stream, as the predetermined reaction time was reached.

The typical parameters and conditions for the carbothermic reduction are as follows: argon flow rate, 0.50×10^{-5} m^3 s^{-1}(298 K, 1.01325×10^5 Pa); sample height, 0.50×10^{-2} m, sample diameter, 0.02 m; reaction temperature, 1,180 to 1,353 K; initial molar ratio of C/ZnS, 2.0; initial molar ratio of CaO/ZnS, 1.5; average size of ZnS, 5.98×10^{-6} m; average size of carbon aggregate, 67.7×10^{-6} m; average size of CaO, 17.90×10^{-6} m; initial bulk density, 429.1 kg m^{-3}; reaction time 450–10,800 s (0.125–3 h).

2.4. Analysis by XRD

Samples for XRD analysis were ground by a mortar and a pestle to fine powders. A Rotaflex Ru-200B diffractometer (Rigaku Co., Tokyo, Japan) was used for XRD analysis and copper K_α radiation was generated at an acceleration voltage of 4.0×10^4 V and a current of 100 mA. The diffraction angle was varied from 20 to 100 deg at a rate of 0.167 deg s^{-1}.

ZnS, ZnO, CaO and CaS could be detected qualitatively by XRD except carbon due to its amorphous character.

2.5. Analysis by SEM

The morphology of the grains of samples were observed by an SEM (model S360, Cambridge Instruments Ltd., Cambridge, United Kingdom). An accelerating voltage of 20 kV was employed during the analysis.

2.6. Analysis by surface area analyzer

The specific surface area, specific pore volume, and average pore diameter of the solid sample were measured by a surface area analyzer (model ASAP 2010, Micromeritics, Norcross, GA). The specific surface area was determined by Brunauer-Emmett- Teller (BET) method [7], while the specific pore volume and average pore diameter were measured by Barreott-Joyner-Halenda (BJH) method [8]. Each sample was evacuated down to 66.7 Pa at 423 K for at least 43,200 s (12 h) prior to the measurement. Adsorption and desorption isotherms of nitrogen were determined gravimetrically at liquid nitrogen temperature.

2.7. Analysis by laser diffraction particle size analyzer

The particle size distributions of ZnS and CaO were analyzed by a laser diffraction particle size analyzer (model LS-230, Beckman Coulter Co., Miami, Florida). The average sizes of ZnS and CaO were determined to be 5.98×10^{-6} m and 17.90×10^{-6} m, respectively.

3. Results and discussions

3.1. Analysis by XRD

Three series of XRD analyses have been performed. In the first series, XRD has been performed on ZnS, CaO, CaS unheated and heated in argon stream at 1,180, 1,203, 1,253, 1,303 and 1,353 K for 450 s. The XRD patterns of CaO and CaS samples with or without heat treatment are the same. Those for ZnS samples, unheated and heated, are different. Some results are shown in Fig. 1. The significant peaks for the unheated ZnS sample appear at $2\theta = 28.5°$, $47.5°$ and $56.3°$ while those for the heated ZnS sample appear at $2\theta = 26.9°, 28.5°, 30.5°, 39.6°, 47.5°, 51.8°$ and $56.4°$. The peak intensities at $28.5°$, $47.5°$ and $56.3°$ decrease upon increasing the temperature, whereas the intensities of the peaks at $26.9°$, $30.5°$ and $51.8°$ increase. This phenomenon can be explained as follows. The main peaks for β-type and α-type of ZnS found from 5-566 card and 5-492 card of the Joint Committee on Powder Diffraction Standards, JCPDS [9], are $2\theta = 28.557°, 33.088°, 47.513°, 56.287°, 69.519°, 76.803°, 88.545°$ as well as $95.533°$ for β-type and $2\theta = 26.921°, 28.511°, 30.536°, 39.616°, 47.539°, 51.781°, 55.510°, 56.399°, 57.594°, 72.930°, 76.007°, 77.844°, 79.073°, 88.595°$ as well as $91.820°$ for α-type. The peaks of α-type and β-type ZnS overlap each other at $28.5°$, $47.5°$ and $56.3°$. Therefore, the increase of $26.9°$, $30.5°$ and $51.8°$ and the decrease of $28.5°$, $47.5°$ and $56.3°$ observed in the XRD patterns show the transformation of ZnS from β-type to

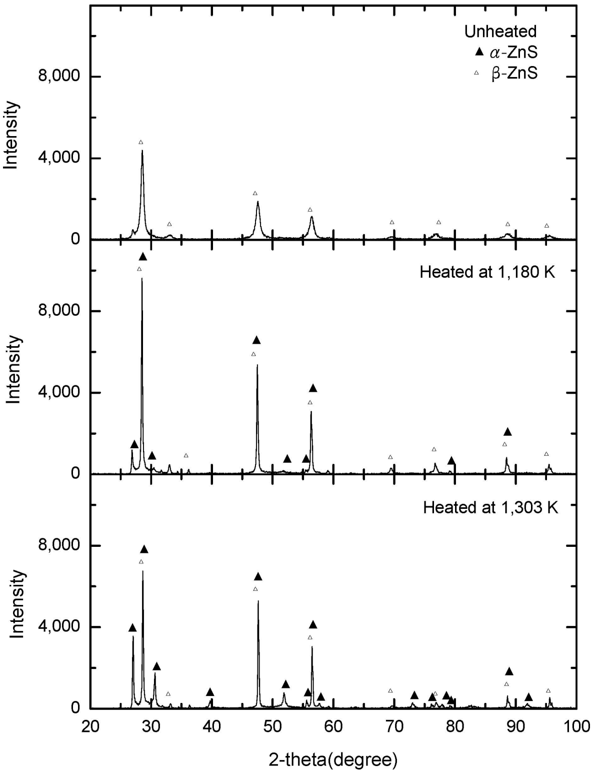

Figure 1 X-ray diffraction patterns of ZnS for various heating temperatures. Heating time = 450 s.

α-type. Fig. 1 implies that β-type ZnS transforms to α-type ZnS starting from 1,180 K and the extent of transformation increases as the temperature increases. This finding of 1,180 K phase transformation temperature is relatively close to the literature value of 1,273 K [4].

The second and third series of XRD analysis were performed on the partially reacted solid sample. Second series was on the sample reacted at 1,303 K for different reaction times: 0, 450, 900, 1,800, 2,700, 3,600, 4,500, 5,400, 7,200, 9,000 and 10,800 s. The XRD patterns for 450, 2,700, 4,500 and 7,200 s are depicted in Fig. 2. The diffraction peaks of ZnS, ZnO, CaO and CaS can be observed in the figures while those of Zn and C are not. The reasons are that Zn was vaporized and C was in the amorphous form. The peak intensities of ZnS (26.92 deg), ZnO (36.25 deg), CaO (37.35 deg) and CaS (31.41 deg) determined from these patterns were plotted against time and the results are shown in Fig. 3. The results depicted in this figure can only provide us with the information of the growth or reduction of a specific substance during reaction. Accordingly it is observed that the amounts of ZnS and CaO decrease monotonically with time, since they are the reactants while that of CaS increases monotonically because it is the final product. The most interesting finding from Fig. 3 is that small amount of ZnO, which has never been added, was found in the solid sample. The amount of it was found to increase with reaction time, reach a maximum at about 1,800 s (0.5 h) and then decrease. The existence of ZnO and the variation of the amount of it indicate that ZnO is an intermediate product of Reaction 1 [10]. Based on the findings presented above, it is known that the transformation sequence of zinc compounds during reaction is ZnS (s, β-type) → ZnS (s, α-type) → ZnO (s) → Zn (g).

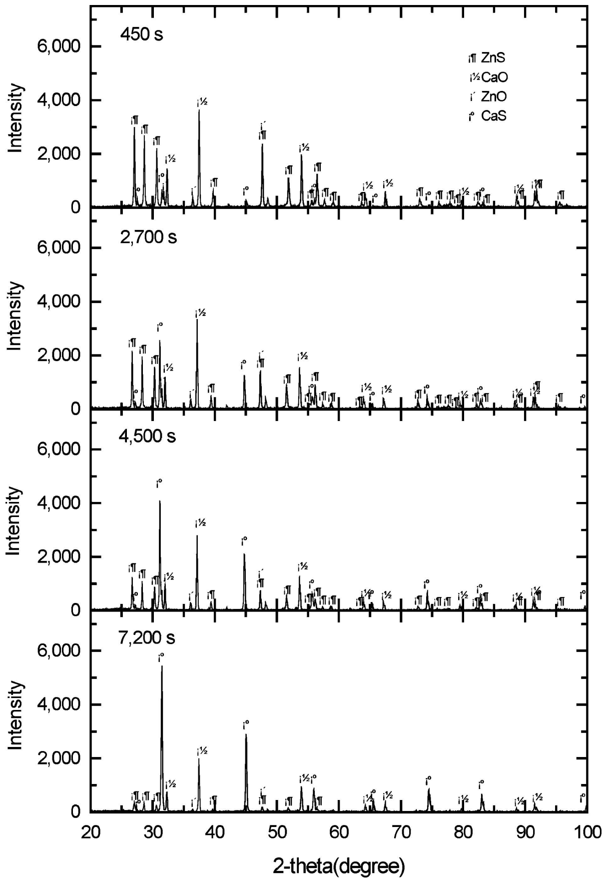

Figure 2 X-ray diffraction patterns of solid samples partially reacted for various times. Reaction temperature = 1,303 K.

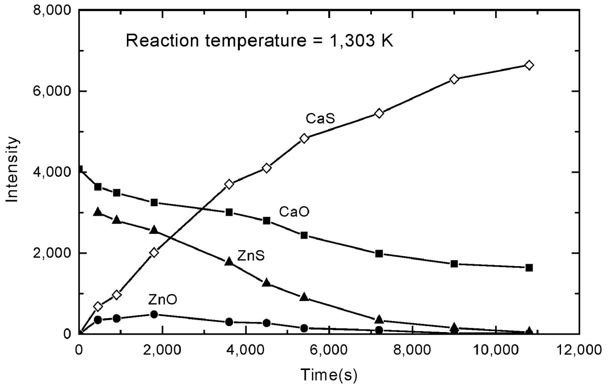

Figure 3 Variations in the intensities of XRD peaks of ZnS, ZnO, CaO, and CaS as a function of reaction time. Reaction temperature = 1,303 K.

In the third series of XRD measurements, the analysis was performed on the solid samples reacted at 1,180, 1,203, 1,253, 1,303 and 1,353 K for 10,800 s (3 h). The variations in the intensities of ZnS, ZnO, CaO and CaS, obtained from XRD patterns are depicted in Fig. 4. The amount of ZnS at 1,180 K is not given because ZnS is still in β-type at this temperature. Fig. 4 indicates that there are still large amounts of reactants, ZnS and CaO, in the solid sample when the reaction temperature is lower than 1,203 K. At the same time, only a small amount of product, CaS, appears. As the temperature is above 1,253 K, the amounts of ZnS and CaO drop and that of CaS increases rapidly. This means that the

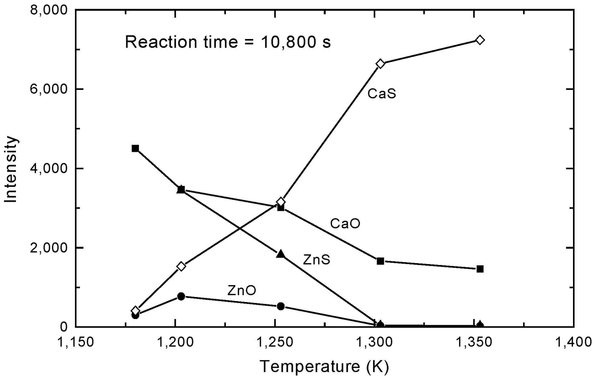

Figure 4 Variations in the intensities of XRD peaks of ZnS, ZnO, CaO, and CaS as a function of reaction temperature. Reaction time = 10,800 s.

reaction is slow for temperatures lower than 1,203 K and fast for temperatures higher than 1,253 K. The amount of the intermediate product ZnO is small at 1,180 K, maximum at 1,203 K, low at 1,253 K and disappears at 1,353 K.

Since the variations of the amounts of ZnS, ZnO, CaO and CaS with reaction time and temperature cannot be found in the literature, a comparison of present results with literature values is not possible.

3.2. Analysis by SEM

Fig. 5 shows the SEM micrographs of ZnS, CaO, C and the unreacted solid sample. Fig. 5a reveals that ZnS grain has a dense and "popcorn-like" shape. About ten grains aggregate into an agglomerate. The diameter of the grain is in the range of $1.0 \times 10^{-6} - 3.0 \times 10^{-6}$ m. The diameter of the agglomerate ranges from $5.0 \times 10^{-6} - 10.0 \times 10^{-6}$ m, as compared to 5.98×10^{-6} m determined by the laser diffraction particle size analyzer. From Fig. 5b it may be seen that CaO grain has a rectangular or diamond slab shape with length and width ranging from 8.0×10^{-6} to 15.0×10^{-6} m. Three or four CaO grains aggregate together and the size of the agglomerate is about 20.0×10^{-6} m. The average size of CaO determined by the laser diffraction particle size analyzer was 17.90×10^{-6} m. The sizes of ZnS and CaO determined by SEM and laser diffraction particle size analyzer are close to each other. The carbon grains shown in Fig. 5c are very fine. The approximate size is in the range of $0.5 \times 10^{-6} - 1.0 \times 10^{-6}$ m. The grains are capable of aggregating easily to form a large agglomerate. The grains of ZnS, CaO and C in the unreacted sample can be easily distinguished based on the shape and size observed in their own electron micrographs.

The electron micrographs of solid samples reacted at 1,303 K for 450, 4,500, and 10,800 s are given in Fig. 6. It can be seen that zinc containing grains become small and few as the reaction proceeds due to zinc evaporation. It is also observed that calcium containing grains become large and round upon increasing the reaction time owing to the transformation of CaO to CaS (true molar density of CaO is 0.06 kmol m^{-3} and that of CaS is 0.0347 kmol m^{-3} [11]) and the sintering of CaO and

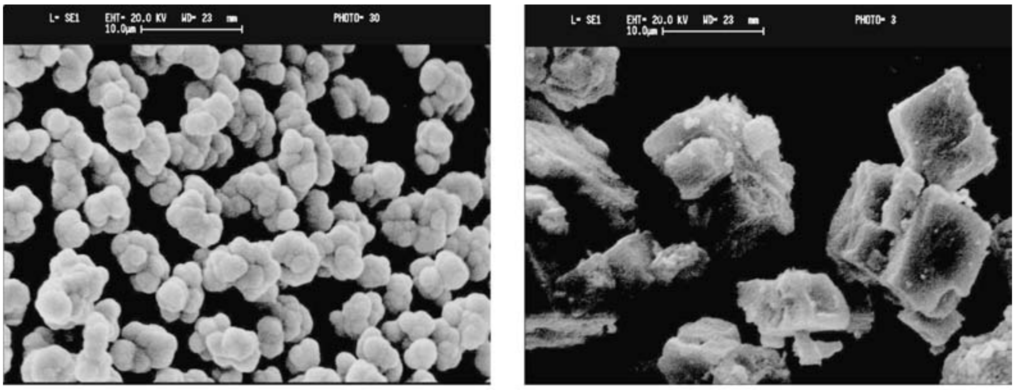

(a) ZnS (b) CaO

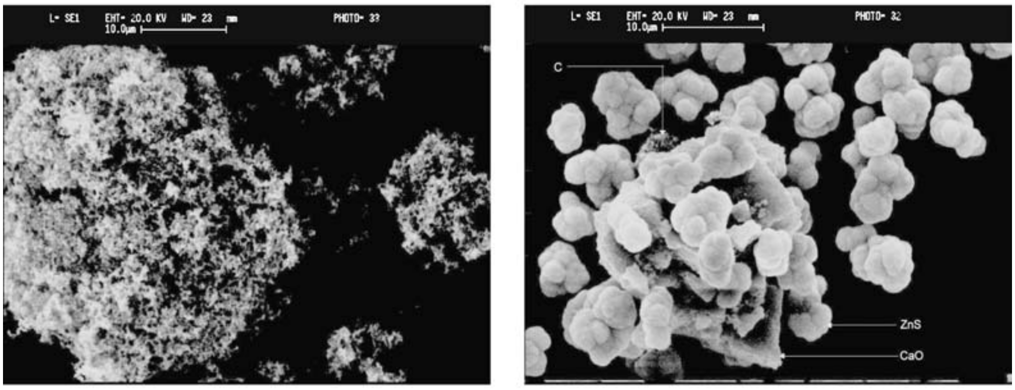

(c) C (d) unreacted sample

Figure 5 Scanning electronmicrographs of (a) ZnS, (b) CaO, (c) carbon black and (d) unreacted sample.

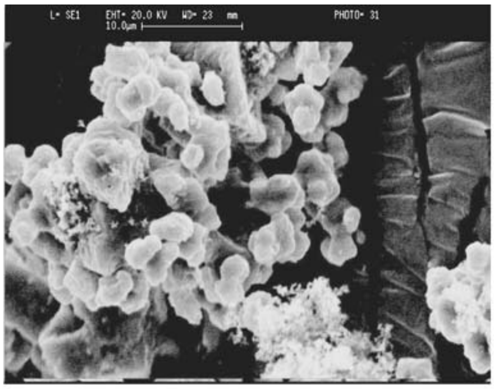

(a)450 s

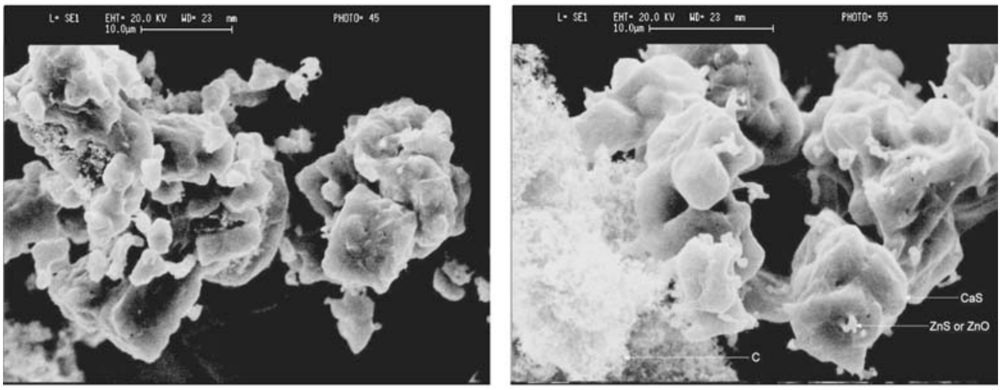

(b) 4,500 s (c) 10,800

Figure 6 Scanning electronmicrographs of solid samples. Reaction temperature = 1,303 K. (a) 450 s, (b) 4,500 s and (c) 10,800 s.

CaS. The variation of carbon grain cannot be observed easily from these pictures. As time reaches 10,800 s, the reaction goes to an end. But, carbon grains still can be found in Fig. 6c. This is due to the excess amount of *C* added to the unreacted sample.

Fig. 7 shows the SEM micrographs of solid samples reacted at 1,180, 1,203, 1,253 and 1,353 K for 10,800 s (3 h). It can be noted from Figs 7a and b that large amount of ZnS is still left and the shape as well as size of calcium containing particles are unchanged at 1,180 and 1,203 K. The pictures in Figs 7c and d, however, shows that zinc containing grains become small and few and calcium containing grains become large and round for 1,253 and 1,353 K. The above results imply that the degree of reaction and sintering is slow when the temperature is less than 1,203 K and become severe when it is above 1,253 K. These results coincide with those of XRD.

3.3. Analysis by surface area analyzer

The results of the measurements of surface area analyzer are presented in Figs 8 and 9. The variations of total surface area, total pore volume, and average pore diameter of a solid sample reacted at 1,303 K with reaction time are given in Fig. 8. The total surface area was found to be reduced abruptly at the initial stage and increased with time in the later stage. The total pore volume dropped drastically in the initial stage and increased gradually later on. The average pore diameter, however, was observed to be increased remarkably in the initial stage, decreased with time monotonically and then leveled off in the later stage. These observations can be explained in the following way. In the first stage when time was less than 450 s, the reductions in the total surface area and total pore volume as well as the increase in the average pore diameter were due to the phase transformation of ZnS. In the second stage, 450-7, 200 s, in which reaction and sintering were rigorous, changes of these physical properties are due to (1) zinc vapor evolution, (2) carbon gasification, (3) volume expansion of CaS and (4) sintering. The effects of these factors on the variations of physical properties are depicted in Table I. It indicates the fact that zinc vapor evolution increases the total surface area, total pore volume and average pore diameter. Carbon gasification has similar effects. Volume expansion of CaS, however, increases the total surface area and reduces total pore volume as well as the average pore diameter. The last

TABLE I Effects of zinc vapor evolution, carbon gasification, volume expansion of CaS and sintering on total surface area, total pore volume and average pore diameter

	Total surface area	Total pore volume	Average pore diameter
1. Zinc vapor evolution	↑	↑	↑
2. Carbon gasification	↑	↑	↑
3. Volume expansion of CaS	↑	↓	↓
4. Sintering	↓	↓	↓

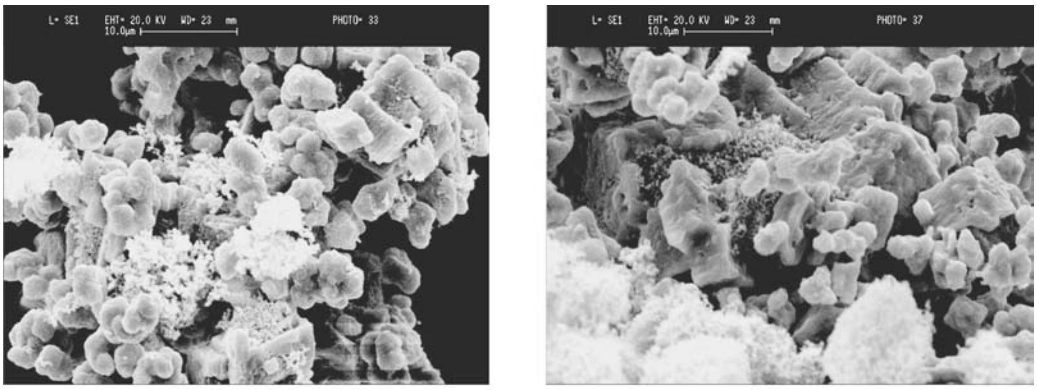

(a) 1,180 K (b) 1,203 K

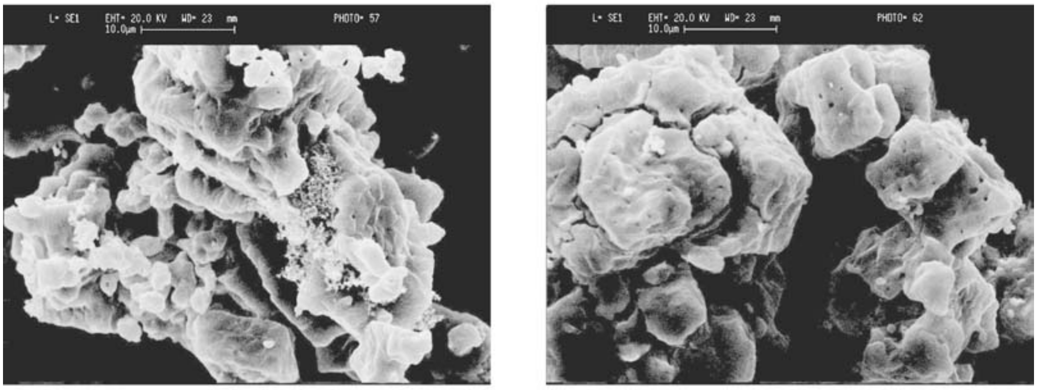

(c) 1,253 K (d) 1,353 K

Figure 7 Scanning electronmicrographs of solid samples. Reaction time = 10,800 s. (a) 1,180 K, (b) 1,203 K, (c) 1,253 K and (d) 1,353 K.

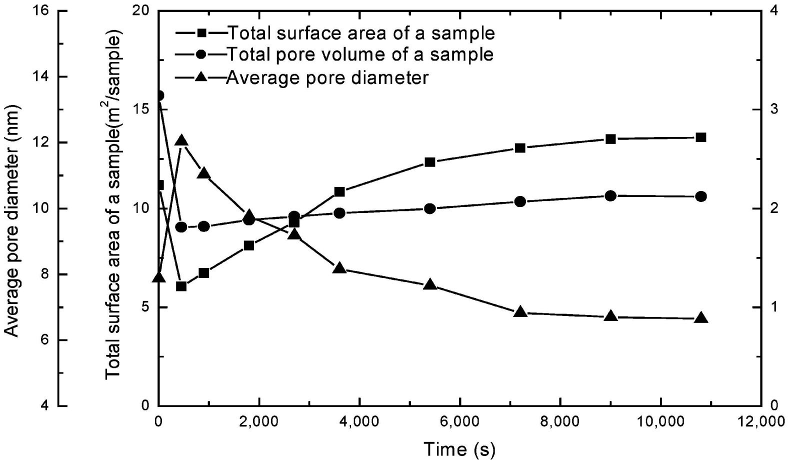

Figure 8 Plots of total surface area, total pore volume and average pore diameter of a partially reacted solid sample against reaction time, respectively. Reaction temperature = 1,303 K.

factor, sintering, decreases the values of these physical properties. If the focus is on the column of total surface area, it is obvious that total surface area is increased by the first factor, zinc vapor evolution; second factor, carbon gasification; and third factor, volume expansion of CaS. But, it is decreased by the fourth factor, sintering. The net effect is that it is increased as reaction proceeds as shown in Fig. 8. As to the total pore volume, it is increased by first and second factors and decreased by third and fourth factors. The net effect shown in Fig. 8 is that it is increased mildly with time. The effects of four factors on the change of value of average pore diameter is the same on that of total pore volume. However, the net effect depicted in Fig. 8 is different. That means, the effects of latter two factors are more significant than those of the former two.

In the final stage, 7,200 to 10,800 s, the reaction and sintering came to an end. Hence, the variations of the physical properties are very mild as shown in Fig. 8.

The variations of the physical properties mentioned above with reaction temperature are shown in Fig. 9. It may be observed from this figure that the total surface area increases, total pore volume does not change, while the average pore diameter decreases upon increasing

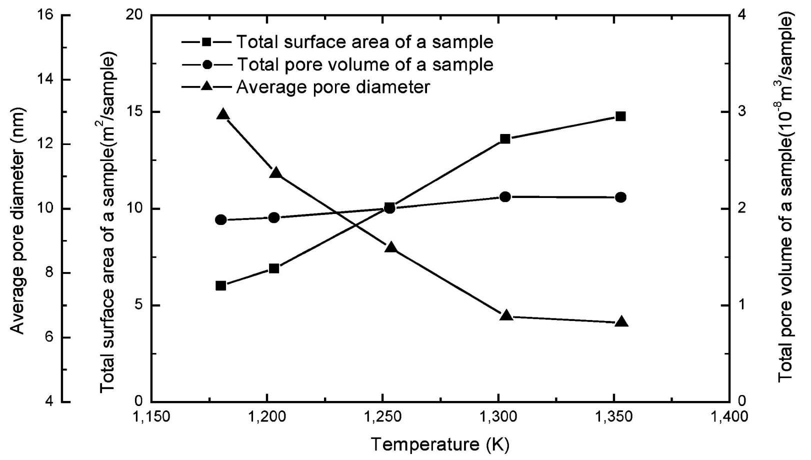

Figure 9 Plots of total surface area, total pore volume and average pore diameter of a partially reacted solid sample against reaction temperature, respectively. Reaction time = 10,800 s.

the temperature. These findings can be explained differently in three temperature ranges. In the range of 1,180 to 1,203 K, the carbothermic reduction and sintering is not severe. Hence, the variations of the physical properties are mild. When the reaction temperature is between 1,203 K and 1,303 K, the reaction and sintering are rigorous. Therefore, the changes in the physical properties excluding total pore volume are pronounced. When the temperature is above 1,303 K, the reaction is over such that the variations of the physical properties are negligible.

A comparison of present results obtained with those reported in literature is impossible because surface area analyzer has never been employed in the study of this reaction system before.

3.4. Reaction mechanism and reaction model

Two mechanisms for Reaction 1 has been proposed in literature. The first one indicates that COS(g) is the intermediate product [1, 3]

$$ZnS(s) + CO(g) = Zn(g) + COS(g) \quad (2)$$

$$CaO(s) + COS(g) = CaS(s) + CO_2(g) \quad (3)$$

$$CO_2(g) + C(s) = 2CO(g) \quad (4)$$

and the second one presumes that ZnO(s) is the intermediate product [4]

$$ZnS(s) + CaO(s) = ZnO(s) + CaS(s) \quad (5)$$

$$ZnO(s) + C(s) = Zn(g) + CO(g) \quad (6)$$

$$ZnO(s) + CO(g) = Zn(g) + CO_2(g) \quad (7)$$

The existence of ZnO in the XRD analysis of the present study (Fig. 3) supports the second mechanism. However, this mechanism should be modified for the following reason. Reaction 6 is a solid/solid reaction and is very slow. As the product gas CO is generated, coupled gas/solid reactions, Reactions 7 and 8, take place immediately.

$$ZnO(s) + CO(g) = Zn(g) + CO_2(g) \quad (7)$$

$$C(s) + CO_2(g) = 2CO(g) \quad (8)$$

The rate of gas/solid reaction is normally much faster than that of solid/solid reaction. Therefore, Reaction 6 is only important in the initial stage while Reactions 7 and 8 are much more significant than Reaction 6 in the propagation stage [12].

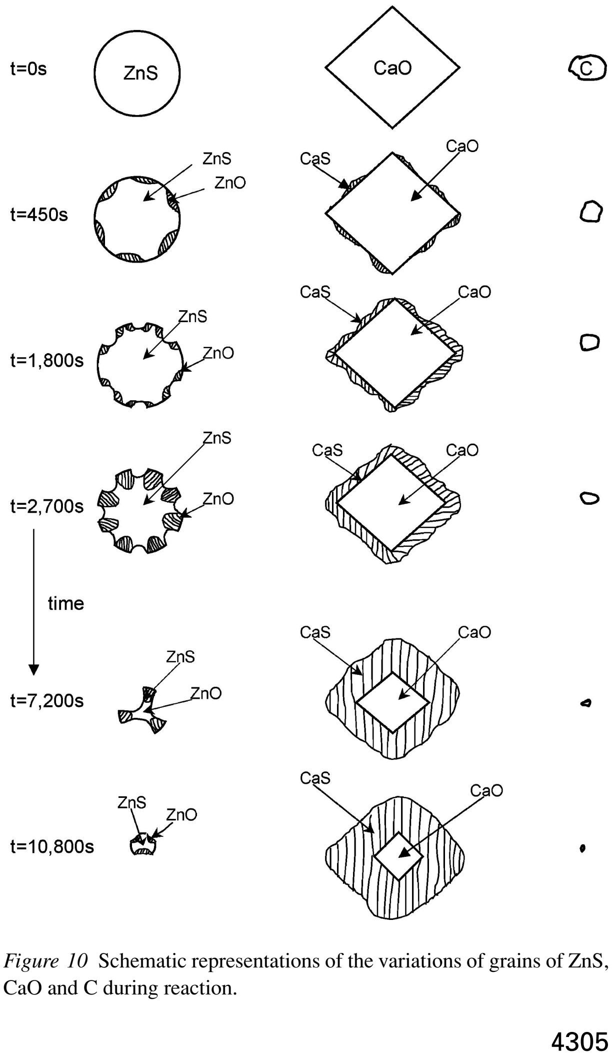

Figure 10 Schematic representations of the variations of grains of ZnS, CaO and C during reaction.

In summary, the probable mechanism for Reaction 1 is

$$ZnS(s) + CaO(s) = ZnO(s) + CaS(s) \quad (5)$$

$$ZnO(s) + C(s) = Zn(g) + CO(g) \quad (6)$$

$$ZnO(s) + CO(g) = Zn(g) + CO_2(g) \quad (7)$$

$$C(s) + CO_2(g) = 2CO(g) \quad (8)$$

Of these reaction steps, Reaction 5 is considered as the rate limiting step since it is a solid/solid reaction and Reaction 6 is insignificant in the propagation stage. Moreover, the very long time for the complete reaction (9,000–10,800 s (2.5–3 h)) supports this. Ueda *et al.* [4] also have similar proposition.

Based on the experimental results of XRD, SEM and surface area analyzer, a reaction model is sketched in Fig. 10 to interpret the variations of composition and morphology of the solid sample during reaction. This figure shows that as time progresses, part of ZnS is oxidized to ZnO which is, then, reduced to zinc vapor and evolved while calcium oxide containing grain reacts to form CaS and becomes round and the carbon particle diminishes.

4. Summary and Conclusions

1. ZnS in the solid sample first transforms from β-type to α-type initially, reacts to produce an intermediate product, ZnO, and is finally reduced carbothermically to zinc vapor which evolves from the solid matrix as reaction proceeds. Sulfur content is scavenged to CaS remaining in the solid sample and carbon grain is gasified during the reaction.

2. Zinc containing particle and carbon grain diminishes while calcium containing particle swells and rounds off as the reaction proceeds.

3. The total surface area and total pore volume of a solid sample drop abruptly in the beginning stage and then increase while the average pore diameter increases remarkably in the initial stage and then reduces monotonically as time goes on.

4. The rate of reaction seems to be low when the temperature is less than 1,203 K and is high, above 1,253 K.

5. A reaction mechanism and model are proposed to interpret the overall process.

Acknowledgment

The authors are grateful to National Science Council of Taiwan for financial support (NSC 91-2214-E-011-014).

References

1. H. ABRAMOWITZ and Y. K. RAO, *Trans. Inst. Min. Metall. (Sec. C)* **87** (1978) 180.
2. H. C. HSU, MS Thesis, "Department of Chemical Engineering," (National Taiwan University of Science and Technology, Taipei, Taiwan, 2001).
3. G. V. SKOPOV, G. P. KHARITIDI and A. I. TIKHONOV, *Izv. Vyssh. Ucheb. Zaved., Tsvet. Metally.*, (4), 33; *Chem. Abstr.* **85**, (1976) 33.
4. Y. UEDA, T. NAKAMURA and F. NOGUCHI, *J. Min. Met. Jpn.* **99** (1983) 127.
5. C. ZHANG, I. ASAKURA and O. OGAWA, *J. Min. Met. Jpn.* **104** (1988) 469.
6. C. ZHANG, I. ASAKURA and O. OGAWA, *J. Min. Met. Jpn.* **104** (1988) 837.
7. S. BRUNAUER, P. EMMETT and E. TELLER, *J. Amer. Chem. Soc.* **60** (1938) 309.
8. E. P. BARRET, L. G. JOYNER and P. P. HALENDA, *J. Amer. Chem. Soc.* **73** (1951) 373.
9. JOINT COMMITTEE ON POWDER DIFFRACTION STANDARDS, *Powder Diffraction File, Card 5-566, Card 37-1497, Card 5-492, Card 8-464, Card 4-836, Card 5-664*, International Center for Diffraction Data, Swarthmore, PA 1990.
10. H. S. FOGLER, "Elements of Chemical Reaction Engineering," 3rd ed. (Prentice Hall PTR, Upper Saddle River, New Jersey, 1999).
11. R. C. WEAST, "Handbook of Chemical and Physics" (The Chemical Rubber CO., Cranwood Parkway, Cleveland, Ohio, 1971).
12. Y. K. RAO and B. P. JALAN, *Metallurg. Soc. CIM* **4** (1977) 1.

Received 23 February 2004
and accepted 11 March 2005